AAPS PharmSciTech, Vol. 14, No. 1, March 2013 (© 2013)
DOI: 10.1208/s12249-013-9921-9

Research Article

Thermally Triggered Mucoadhesive *In Situ* Gel of Loratadine: β-Cyclodextrin Complex for Nasal Delivery

Reena M. P. Singh,[1] Anil Kumar,[1,2] and Kamla Pathak[1]

Received 26 July 2012; accepted 7 January 2013; published online 29 January 2013

Abstract. The aim of the present study was to increase the solubility of an anti-allergic drug loratadine by making its inclusion complex with β-cyclodextrin and to develop it's thermally triggered mucoadhesive *in situ* nasal gel so as to overcome first-pass effect and consequently enhance its bioavailability. A total of eight formulations were prepared by cold method and optimized by 2^3 full factorial design. Independent variables (concentration of poloxamer 407, concentration of carbopol 934 P, and pure drug or its inclusion complex) were optimized in order to achieve desired gelling temperature with sufficient mucoadhesive strength and maximum permeation across experimental nasal membrane. The design was validated by extra design checkpoint formulation (F9) and Pareto charts were used to help eliminate terms that did not have a statistically significant effect. The response surface plots and possible interactions between independent variables were analyzed using Design Expert Software 8.0.2 (Stat Ease, Inc., USA). Faster drug permeation with zero-order kinetics and target flux was achieved with formulation containing drug: β-cyclodextrin complex rather than those made with free drug. The optimized formulation (F8) with a gelling temperature of 28.6±0.47°C and highest mucoadhesive strength of 7,676.0±0.97 dyn/cm^2 displayed 97.74±0.87% cumulative drug permeation at 6 h. It was stable for over 3 months and histological examination revealed no remarkable damage to the nasal tissue.

KEYWORDS: 2^3 factorial design; *in situ* nasal gel; loratadine; mucoadhesion; temperature-induced gelation.

INTRODUCTION

Loratadine (LOR) is a second-generation antihistaminic drug used in treatment of allergies such as hay fever (allergic rhinitis), urticaria (hives), upper respiratory tract infections, and other skin allergies (1). Loratadine, when given orally, is well absorbed from the gastrointestinal tract and reaches peak plasma levels within 1–1.5 h (2). It undergoes rapid first-pass hepatic metabolism which leads to poor oral bioavailability of 40% (3). Thus to bypass the liver, an alternative route of administration would be preferred.

Transmucosal routes of drug delivery offer the advantages of possible bypass of first-pass effect and avoidance of presystemic elimination of gastrointestinal tract. Therapeutic effect may be achieved in smaller dose of a particular drug (4). Intranasal drug delivery is a promising transmucosal route for administration of drugs as it possesses all the above-listed advantages, has large absorptive surface area with high vascularity (5), and is considered equivalent to i.v. route. However, the disadvantage associated with the nasal route is rapid elimination of the instilled drug from the nasal cavity by mucociliary beating (clearance half-life of 15 min). This limits the time available for drug absorption from the applied dosage form and thus results in poor nasal bioavailability. In order to prevent rapid mucociliary clearance and improve the bioavailability, a mucoadhesive system may be utilized. These systems adhere onto the mucus and increase the residence time within the nasal cavity. This intensifies contact between nasal mucosa and the drug and facilitates the drug absorption which results in increased bioavailability (6).

Mucoadhesive microspheres of LOR for nasal delivery have been reported where the researchers ensured longer retention time of ethylcellulose microspheres at the site of deposition and avoidance of hepatic metabolism resulting in improved bioavailability. However, the rigid nature of microspheres has potential of sneezing or causing obstruction of nasal airway pathway (7). Thus, the present project was aimed at avoidance of multiparticulate system for nasal delivery to avoid the listed complications and consequently to develop a thermally triggered mucoadhesive *in situ* nasal gel in which the drug (solubilized form) is directly dispersed in the polymeric dispersion of LOR. This delivery system is expected to overcome the limitation of earlier report and couple the advantages of mucoadhesion along with the nasal delivery. Poloxamer 407 was selected as a thermosensitive gelling polymer because it has low toxicity and irritation, excellent water solubility, and compatibility with most of the proposed formulative excipients (8). For the mucoadhesive property, carbopol 934 P was used which increases viscosity of the formulation and forms hydrogen bond with the mucosa that increases the nasal residence time of the formulation (6).

[1] Department of Pharmaceutics, Rajiv Academy for Pharmacy, NH# 2, P.O. Chhatikara, Mathura, 281001, Uttar Pradesh, India.
[2] To whom correspondence should be addressed. (e-mail: anilsoni.n@gmail.com)

Thus, the project will be dual approached: (1) to improve the solubility of a poorly soluble, lipophilic drug loratadine by making its inclusion complex with β-cyclodextrin, and characterize it by scanning electron microscopy (SEM) and spectral techniques; and (2) to formulate an *in situ* nasal gel by incorporating pure drug or inclusion complex of a pure drug, so as to analyze the effect of β-cyclodextrin in drug loading and permeation of the drug across the nasal mucosa. Formulations will be prepared using 2^3 full factorial design wherein four formulations will be made from pure drug while rest of the four formulations will be made with inclusion complex of the drug.

MATERIALS AND METHODS

Materials

Loratadine was a kind gift from Arti Pharmaceuticals, Surat, India. Poloxamer 407 was purchased from BASF, USA. Carbopol 934 P was purchased from Central Drug House, New Delhi. β-cyclodextrin was purchased from International Specialty Product ltd, USA. Potassium bromide was obtained from Spectrochem Pvt. Ltd., Mumbai, India. All other ingredients used were of analytical grade.

Methods

Phase Solubility

Phase solubility study of LOR, in the presence of β-CD was carried out in double-distilled water at 25±0.5°C according to the method described by Higuchi and Connors (9). Aqueous solutions (10 ml) of different concentrations of β-CD were prepared and an excess amount of LOR was added separately and then shaken for 72 h. After 72 h, the suspensions were filtered through 0.45-μm membrane filter. A 50% *v*/*v* ethanolic water was used for the appropriate dilution of each filtrate and assayed against the blank prepared by using different concentrations of β-CD in distilled water and measured by UV spectrophotometer at 260 nm (Shimadzu Pharmaspec 1700, Kyoto, Japan). The apparent stability constant (K) was calculated from the slope and intercept of the straight line of the phase solubility diagram, according to the following Eq. (1):

$$K = \text{slope}/S_0(1 - \text{slope}) \quad (1)$$

S_0=intrinsic solubility of LOR in the absence of β-CD or intercept of phase solubility diagram

Preparation of Solid Inclusion Complex of LOR and β-CD

The solid inclusion complex of LOR and β-CD in 1:1 molar ratio was prepared by kneading method. β-CD was impregnated with adequate amount of ethanol (95% *v*/*v*) to convert it into a paste. LOR was then added to the above paste and kneaded thoroughly with a pestle for 15 min, and dried at 50°C for 24 h. The resultant dry solid mass was powdered and passed through a 60-mesh sieve and stored in dessicator until use.

Equilibrium Solubility

Ten mg of drug and its complex with β-CD equivalent to 10 mg of drug were added separately to 10 ml of distilled water in a conical flask and kept for 72 h at 37°C on water bath shaker (HICON Enterprises, New Delhi, India). Aliquot samples were withdrawn periodically, filtered through membrane filter (0.45 μ) and analyzed spectrophotometrically.

Characterization of Raw Materials and Solid Inclusion Complex of LOR

Scanning Electron Microscopy

The photomicrographs of LOR, β-CD, LOR/β-CD complex, and physical mixture of LOR and β-CD were obtained using scanning electron microscope (JEOL 5400, Tokyo, Japan) operated at an acceleration voltage of 10 kV. The samples were prepared by adhering the powder on a double-sided tape stuck to aluminum stub. The stubs were then coated with thin gold layer by sputter coater unit (VG Microtech, West Sussex, UK) under argon atmosphere in order to make them conductive and the surface morphology of samples was studied by observing at ×2,000 magnification.

Differential Scanning Calorimetry

Differential scanning calorimetry (DSC) profiles of LOR, β-CD, LOR/β-CD complex, and physical mixture of LOR and β-CD were obtained using Perkin Elmer DSC 7, USA. Thermal behaviors were studied under normal conditions with samples sealed in silver pans and with a nitrogen gas flow of 20 ml/min. The heating rate of the samples was 10°C/min over a temperature range of 40–300°C.

Fourier Transformed-Infrared Spectroscopy

LOR, β-CD, LOR/β-CD complex, and physical mixture of LOR and β-CD were examined using Fourier transformed-infrared spectroscopy (FTIR) spectrophotometer (Shimadzu FTIR-8400S Kyoto, Japan). The test sample diluted with KBr, to get a final dilution of 1:10, was mounted into the sample holder. The measurements were made in transmittance mode in the range of 500–4,000 cm^{-1} against the background spectra of pure KBr by setting the resolution of 4 $cm^{-1}$and 50 times accumulation.

X-ray Diffractometry

X-ray diffraction pattern of LOR, β-CD, LOR/β-CD complex, and physical mixture of LOR and β-CD were recorded using a D8 Advance X-ray diffractometer (Bruker, Germany). The samples were irradiated with Ni filtered 2.2 kW Cu anode radiation, generated at 1.542 Å wavelength, at 30 kV and 30 mA. Dermic X-ray tube was equipped with a sample holder having Zero Background and PMMA and Lynux Eye detector. The samples were step scanned between 0 and 70° at 2θ scale.

Experimental Design

A 2^3 full factorial experimental design was used to optimize *in situ* nasal gel wherein the concentration of poloxamer (A), concentration of carbopol 934 P (B), and LOR:β-CD/LOR (C) were chosen as independent variables. Each variable set at high level and low level and a total of eight formulations were designed (Table I). Gelling temperature, mucoadhesive strength, and percent cumulative drug permeated at 6 h were taken as dependent variables. Design expert version 8.0.2. (Stat-Ease, Inc, USA) was used to analyze the effect of each variable.

Preparation of Thermally Triggered Mucoadhesive In Situ Nasal Gel

In situ nasal gels were prepared by the cold method described by Schmolka (10). Specified amount of LOR/LOR/β-CD complex and carbopol 934 P were stirred in the calculated amount of distilled water at room temperature. The dispersions were cooled to 4°C by keeping it in a refrigerator. Poloxamer 407 was added slowly with continuous stirring (thermostatically controlled magnetic stirrer, S.M. Scientific Instruments (P), Ltd., India). Dispersions were then stored in a refrigerator overnight to get clear sol and eventually stored in a refrigerator so that it remains in sol form.

Evaluation of *In Situ* Nasal Gel

Gelling Temperature and Time

Two milliliters of each formulation was transferred to a test tube immersed in a water bath. The temperature of was increased in increments of 1°C and left to equilibrate for 5 min at each new setting. The samples were examined for gelation which was said to have occurred when the meniscus would no longer move upon tilting through 90°. Gelling time was recorded as the time for first detection of gelation as defined above.

Table I. 2^3 Full-Factorial Design of Loratadine *In Situ* Nasal Gel and the Dependent Variables

Formulation code	Poloxamer 407 (A) (% *w/v*)	Carbopol 934 P (B) (% *w/v*)	Drug/β-CD (C) (molar ratio)[a]	Dependent variables
F1	18 (−)	0.5 (−)	1 (−)	Gelling temperature
F2	18 (−)	0.5 (−)	1:1 (+)	
F3	18 (−)	1 (+)	1 (−)	Mucoadhesive strength
F4	18 (−)	1 (+)	1:1 (+)	
F5	20 (+)	0.5 (−)	1 (−)	% cumulative drug permeated
F6	20 (+)	0.5 (−)	1:1 (+)	
F7	20 (+)	1 (+)	1 (−)	
F8	20 (+)	1 (+)	1:1 (+)	

[a] Drug=2% *w/v*

pH, Viscosity, and Drug Content

One milliliter of each formulation was transferred to a 10 ml volumetric flask and diluted by double-distilled water to a volume of 10 ml. The pH of resulting solution was determined by calibrated pH meter (111 E; HICON, New Delhi, India). The viscosity of sol was measured using Brookfield viscometer DV-II+ Pro coupled with S-94 spindle at 100 rpm at 4±1°C. For drug content determination, 1 ml of the formulation was extracted with 1 ml of the ethanol (95% *w/v*) by vortexing and diluted with phosphate buffer pH6.4 to 10 ml. The samples were filtered through Whatman filter paper and LOR was assayed spectrophotometrically.

Gel Strength

Gel strength was measured by placing 50 g of formulation in a 100 cm^3 graduated cylinder and gelled at 37°C using thermostat. A piston of weight 35 g was placed onto the gelled solution and allowed to penetrate 5 cm in the gel. Time taken by weight to sink 5 cm was measured (11).

Ex Vivo Mucoadhesive Strength

Ex vivo mucoadhesive strength was determined by modified balance method (Fig. 1) using the freshly cut sheep nasal mucosa procured from local slaughter house. The two sides of the balance were balanced by keeping one beaker on the left hand pan and 5 g weight on the right hand pan. A piece of (1× 1 cm^2) of sheep nasal mucosa was fixed over glass support with cyanoacrylate glue with the mucosal side upwards. The glass support was then lowered into the glass container filled with phosphate buffer pH6.4 to keep the mucosa moist and kept below the right hand side of the balance. One gram of the gel was spread as a thin film (thickness 1 mm) on the lower surface of the right hand pan of the balance. The beaker was removed from the left hand pan which lowered the right hand pan along with the gel. The balance was kept in this position for 2 min contact time. The beaker was replaced on the left hand pan and water was gradually added from burette at the rate of 100 drops/min to the beaker over left hand pan until the mucosal membrane detached from the gel surface (12). The mucoadhesive force expressed as the detachment stress in dynes per square centimeter was determined from the minimal weight that detached the mucosal tissue from surface of each formulation.

$$\text{Mucoadhesive strength}\left(\text{dynes/cm}^2\right) = \text{m} \times \text{g/A} \quad (2)$$

Where, m=weight required for detachment in gram, g=acceleration due to gravity (980 cm/s^2), and A=area of mucosa exposed.

Ex Vivo Permeation

The *ex vivo* permeation study was performed using nasal mucosa collected from slaughter house. The nasal conch was collected in phosphate buffer pH6.4 and washed three times with phosphate buffer pH6.4 and extraneous tissues were removed. The prepared nasal mucosa was mounted on Franz diffusion cell to get a permeation area of 3.14 cm^2. Sixteen

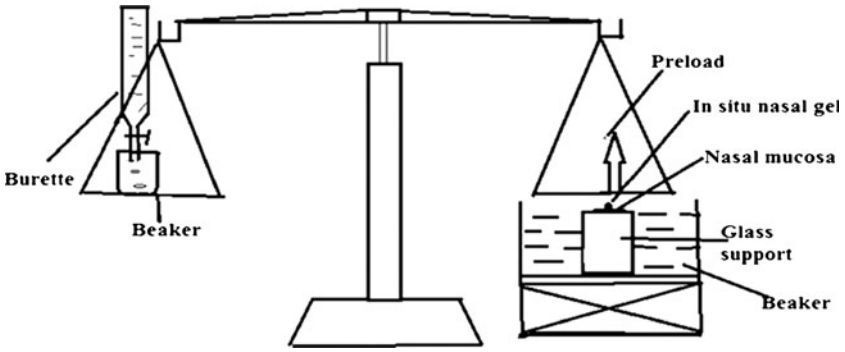

Fig. 1. Laboratory fabricated apparatus used for the determination of mucoadhesive strength of *in situ* nasal gels

milliliters of phosphate buffer pH6.4 was added to the acceptor chamber maintained at 34°C. Formulation equivalent to 10 mg of LOR was placed in the donor chamber. At predetermined time points (0, 30, 60,120, 180, 240, 300, 360, 420, and 480 min), 1-ml sample was withdrawn from the acceptor compartment and replaced with an equal volume of the phosphate buffer pH6.4. The samples were analyzed spectrophotometerically and graphs were constructed between percent cumulative drug permeated *versus* time. Slopes of the linear portion of graphs were used to calculate the flux (in milligram per hour) and permeability coefficient was determined by Eq. 3

$$\text{Permeability coefficient}\,(K_P) = J_{ss} \times 1/C_V \tag{3}$$

Where, J_{ss} is steady state flux (in microgram per square centimeter per hour) and C_v is the total donor concentration of the formulation (in milligram).

The target flux was calculated by Eq. 4

$$(J_{Target}) = C_{ss}CL_TBW/A \tag{4}$$

Where A represents the surface area of the sheep nasal mucosa used for the permeation study, BW represents the standard human body weight of 60 kg, C_{ss} represents the LOR concentration at the therapeutic level (15–27 μg/L), and CL_T represents the total clearance (88–585 ml/min/kg); the average values of both C_{ss} and CL_T were taken to calculate the target flux value of 135.0 μg/cm^2/h for LOR. The permeation kinetics was studied by fitting the data to various kinetic equations (namely zero order, first order, Higuchi, and Peppas) to determine the appropriate kinetic model.

Statistical Analysis of Responses by Design Expert

Design expert 8.0.2 (Stat-Ease Inc., USA) was used to analyze the effect of independent variables on the designated response. Pareto charts were constructed to identify statistically significant response coefficient(s). The transformed polynomial equations generated by Design Expert software were used to validate the design. The design was validated by extradesign check point formulation (F9) by selecting the center point of each variable (Table II). Possible interactions between *AB*, *BC*, and *AC* were also studied.

Selection of Optimized Formulation

The optimized formulation was selected on the basis of least gelling temperature, highest mucoadhesive strength, and highest percent cumulative drug permeated after 6 h with good desirability factor.

Histopathological Study

In histopathological evaluation, nasal tissue used for the *ex vivo* permeation study was compared with freshly collected nasal mucosa incubated with phosphate buffer (pH6.4) to assess damage, if any. At the end of permeation study, the nasal mucosa was cleared off the optimized gel and fixed in 10% buffered formalin (pH7.2), routinely processed and embedded in paraffin. Paraffin sections (7 μm) were cut on glass slides and stained with hematoxylin and eosin. The sections were observed through photomicrograph (Hicon enterprises, New Delhi, India) at ×100 magnification.

Stability Study

For the assessment of stability of optimized *in situ* nasal gel of LOR, the formulation was stored at 40°C/75% relative humidity in the stability chamber for 3 months. The samples were withdrawn at predetermined time intervals of 0, 1, 2 and 3 months and observed for physical stability, drug content, and *ex vivo* drug permeation characteristics.

RESULTS AND DISCUSSION

Phase and Equilibrium Solubility

The phase solubility curve (Fig. 2) revealed linear relationship between apparent solubility of LOR in water as a function of β-CD over the entire concentration range studied.

Table II. Coded Value and Actual Value of Extra Design Check Point Formulation (F9)

Variables	Coded value	Actual value
Concentration of poloxamer 407	0	19% *w/v*
Concentration of carbopol 934 P	0	0.75% *w/v*
Complex of LOR with β-CD	0	1:0.5

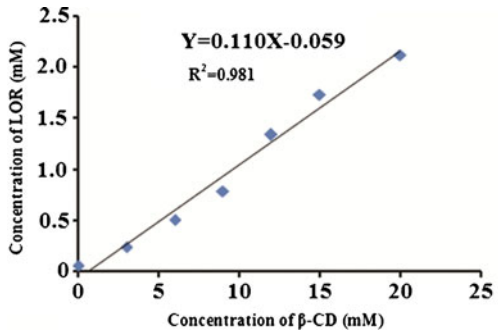

Fig. 2. Phase solubility diagram of LOR with β-CD in double distilled water at 25°C

Linearity was characteristic of A_L-type system and suggested formation of water-soluble complex in solution in 1:1 binding stoichiometry (9). Furthermore, the slope of phase solubility plot was 0.110 that further confirmed formation of inclusion complex in the molar ratio of 1:1. The intrinsic solubility of LOR was found to be 0.059 mM and the apparent stability constant was $2.13\times10^4 M^{-1}$. This value indicates sufficient stability of the complex in solid state that can dissociate to release the drug in solution state. The equilibrium solubility of LOR in double-distilled water was found to be 4.41 μg/ml whereas the solubility of its complex with β-CD was found to be 395.91 μg/ml. Almost 90-fold increase in solubility was due to the formation of amorphous complex.

CHARACTERIZATION OF SOLID INCLUSION COMPLEX OF LOR

Scanning Electron Microscopy

LOR appeared as regular rod like three-dimensional crystals (Fig. 3a) while β-CD appeared as three-dimensional globular particles (Fig. 3b). The physical mixture of LOR and β-CD clearly depicted two separate entities of both LOR and β-CD mixed physically (Fig. 3c). In LOR/β-CD complex (Fig. 3d), the original morphology of both the individual components disappeared. The micrograph revealed absence of crystalline drug and new solid phase as an amorphous product was generated along with few faintly distinguishable LOR crystals.

Differential Scanning Calorimetry

The DSC curve of LOR displayed a sharp endothermic peak at 137.14°C (ΔH=112.78 J/g) due to melting of LOR (Fig. 4a), which is consistent with literature report (13). The thermogram of β-CD (Fig. 4b) revealed a broad endothermic peak at 112.69°C (ΔH=253.62 J/g) which indicates dehydration process and another peak at 265.43°C (ΔH=60.40 J/g) correlatable to decomposition of β-CD (14, 15). The physical mixture of LOR and β-CD was an additive thermogram (Fig. 4c) of endothermic peak at 135.70°C (ΔH=29.03 J/g) for LOR along with a peak of β-CD at 91.90°C (ΔH= 108.56 J/g) and at 275.05°C (ΔH=18.25 J/g). The shift towards lower temperatures was the result of mixing of two components. However, in the DSC curve of LOR/β-CD complex, the characteristic endothermic peak of drug disappeared implying that LOR was included into the cavity of β-CD (Fig. 4d) and a peak for very slight water loss was detectable at 88.91 (ΔH= 103.69 J/g)

FT-IR Spectroscopy

FT-IR spectrum of LOR (Fig. 5a) showed absorption bands for (C≡N stretching) at 2,196.7 cm^{-1}, 1,703.03 cm^{-1} (C=O stretching of ester), 1,571.88, 1,474.09, 1,434.94 cm^{-1} (stretching vibrations of benzene ring, and at 1,228.57 cm^{-1}; C=O stretching of ester) (16). The dominant IR spectral peak for β-CD at 1,647.1 cm^{-1} may be attributed to the –OH groups in the glucose moieties of β-CD (17). Also β-CD could be characterized by the intense band at 3,328.91 cm^{-1} corresponding to vibration of the hydrogen bonded -OH groups as well as the band of 2,931.60 cm^{-1} was assigned to absorption by the –CH and $–CH_2$ groups (Fig. 5b). In the physical mixture of LOR and β-CD, the dominant IR spectral peaks of both LOR and β-CD were observed at 1,703.03 cm−1 (C=O stretching), 1,434.94 cm^{-1} (stretching vibrations of benzene ring, *i.e.*, C=C), 1,228.57 cm^{-1} (C=O stretching of ester) for LOR and 1,647.1 cm^{-1} due to the OH groups in the glucose moieties of β-CD (Fig. 5c). In the FT-IR spectrum of LOR/β-CD complex (Fig. 5d), the characteristic band of C=O stretching of LOR at 1,703.03 cm^{-1} was down shifted to 1,673 cm^{-1} due to inclusion complex formation. The band at 1,433.01 was uppershifted to 1,441 cm^{-1} and C–O stretching at 1,228.57 cm^{-1} was also upper-shifted to 1,230.5 cm^{-1}. Appearance of new spectral peaks explained the inclusion complex formation between LOR and β-CD.

X-ray Diffractometry

The diffractograms of pure LOR exhibited characteristics peaks at 14.60°, 15.52°, 17.04°, 19.42°, 21.06°, 22.63°, 23.42°, 25.02°, 28.03°, and 31.42° due to its crystalline nature (Fig. 6a). β-CD exhibited a series of intense peaks at 5.02°, 9.51°, 10.48°, 11.04°, 13.46°, 14.48°, 16.09°, 19.08°, and 24.08°, which were indicative of crystalline nature of β-CD (Fig. 6b). Most of the principal peaks of LOR and β-CD were present in the diffraction patterns of physical mixture (Fig. 6c). This indicated no interaction between the pure components of physical mixture. In contrast to these observations, LOR/β-CD complex (Fig. 6d) showed disappearance of characteristic peaks of LOR at 19.42°, 21.06°, 22.63°, and 31.42°. Moreover, the peaks were broadened with reduced intensities when compared to pure components (LOR and β-CD). These observations were indicative of the transformation of LOR from crystalline to amorphous state, which might be because of inclusion of LOR into β-CD cavity. Post-characterization, the complex was formulated as thermally triggered *in situ* gel and evaluated for various parameters.

EVALUATION OF THERMALLY TRIGGERED *IN SITU* NASAL GEL

The LOR/β-CD complex and LOR formulated as thermally triggered *in situ* nasal gels were apparently clear. No distinct suspended particles could be observed that may harm nasal mucosa or affect syringeability of the formulations. The gels prepared using complex was more translucent when

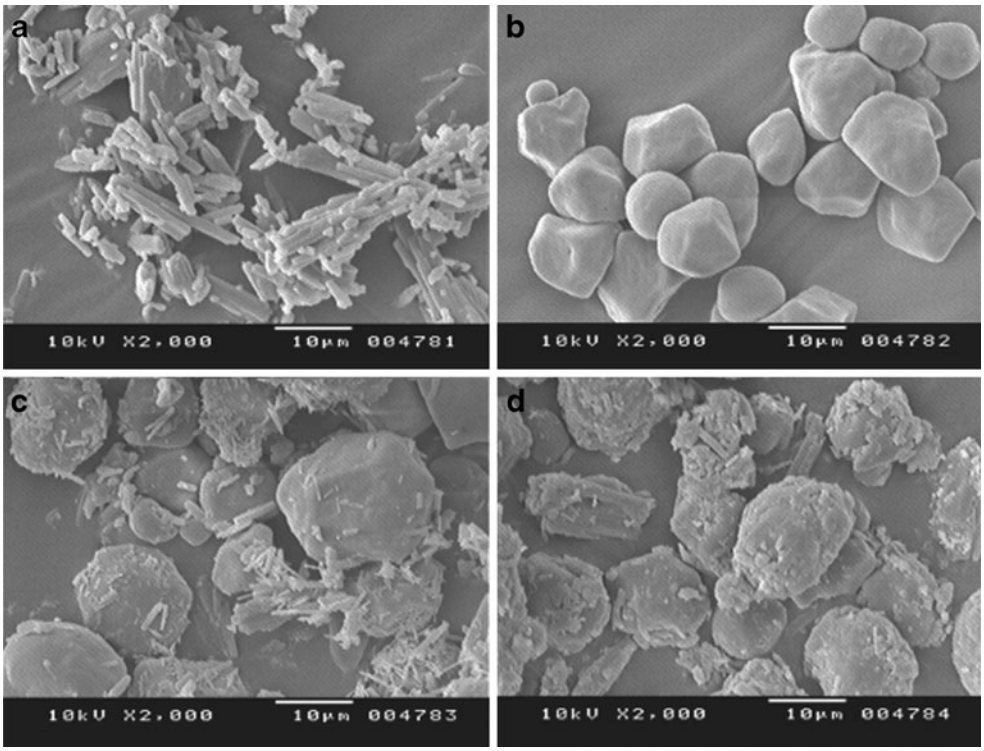

Fig. 3. SEM photomicrograph; **a** pure drug LOR, **b** β-CD, **c** physical mixture of LOR and β-CD, and **d** LOR/β-CD complex

compared to the gels of pure LOR probably due to diffused boundaries of the suspended complex in gel base attributable to its enhanced solubility (9).

Gelling Temperature and Time

The gelling temperature of the formulations ranged between 27.3 and 35.3°C (Table III). A gelling temperature is considered to be suitable in the range of 25–37°C. As at gelling temperature lower than 25°C, a gel might be formed at room temperature leading to difficulty in manufacturing, handling and administering and if it is higher than 37°C, it would not form gel at the temperature of the nasal cavity so results in rapid nasal clearance of administered drug (18). The sols in the study were formulated with block copolymer capable of micellization. When temperature is raised, the number of micelles formed increases due to negative coefficient of solubility of block copolymer micelles. Additionally, the micelles become so tightly packed that the solution becomes immobile and gel is formed (19). Our results revealed that the gelling temperature decreased with increase in the concentration of thermosensitive polymer poloxamer 407 due to formation of larger number of the micelles that occupy large volume at lower temperature (20). Recently, mechanism of gelation-based on micelles association and interactions has been suggested (21). Also, conformational changes in the orientation of the methyl groups in the side chains of poly(oxypropylene) chains, constituting the core of the micelle, with removal of the water from the micelles have also been reported to contribute to the gelation phenomenon (22). The mucoadhesive agent, carbopol 934 P also causes lowering of gelling temperature because of its ability to bind to poly (ethylene) oxide chains present in poloxamer 407 molecule, thus promoting dehydration and causing an increase in entanglement of adjacent molecules with more extensive intermolecular hydrogen bonding and enhanced micellar association (18).

pH, Viscosity, and Drug Content

The nasal mucosa can tolerate formulations in pH of range 3–10. An alkaline pH can inactivate the lysozyme secreted by nasal cells and make the nasal tissue susceptible to microbial infection whereas lower pH acts as a hypertonic solution causing shrinkage of epithelial cells and also inhibits ciliary activity (23, 24). The pH of the formulations narrowly ranged from 5.3 to 5.8 and hence are expected to be free from pH-associated deleterious effects (24). The thermally triggered nasal formulations should have an optimum viscosity so that it can easily pass through needle of 23 or 27 gauge, for easy administration into the nasal cavity, as a liquid that will undergo rapid sol to gel conversion. The viscosity of the formulations ranged between 27.3 and 43.6 cps (Table III). A marked increase in viscosity was observed in the formulations made with high amount of carbopol 934 P (F3, F4, F7, and F8), a viscosity enhancing polymer that aids in increasing nasal residence time. The drug content varied from 75.2 to 98.91% (Table III) and the formulations (F2, F4, F6, and F8) containing β-CD complex of LOR had higher drug content than the formulations with pure LOR. This may be due to increase in solubility of drug, which caused higher loading of drug in the *in situ* gel that resulted in almost 100% drug loading in formulations made with complex.

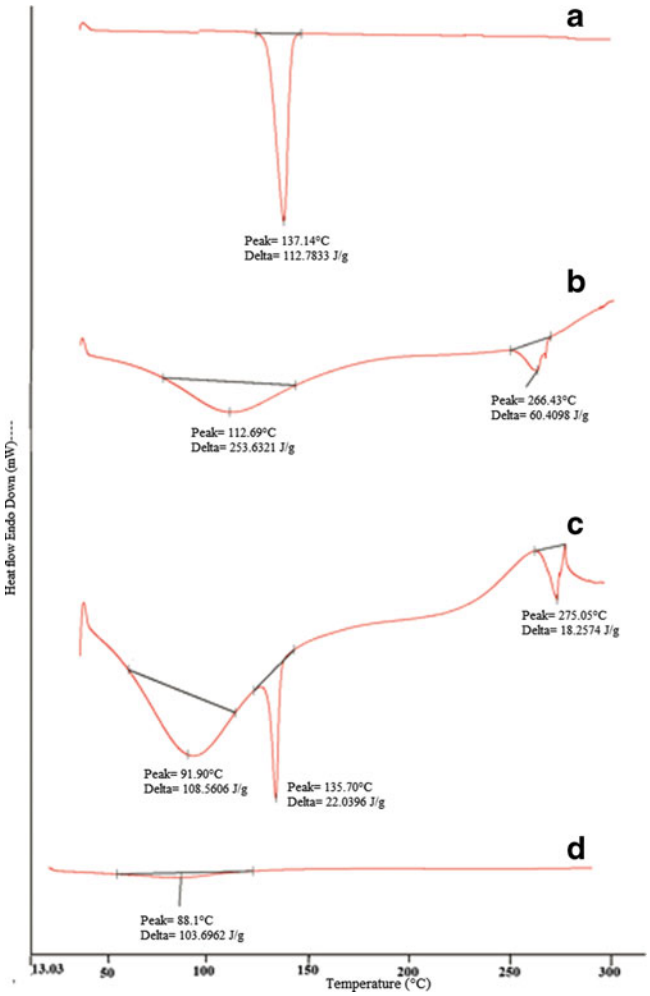

Fig. 4. DSC; *a* pure drug LOR, *b* β-CD, *c* physical mixture of LOR and β-CD, and *d* LOR/β-CD complex

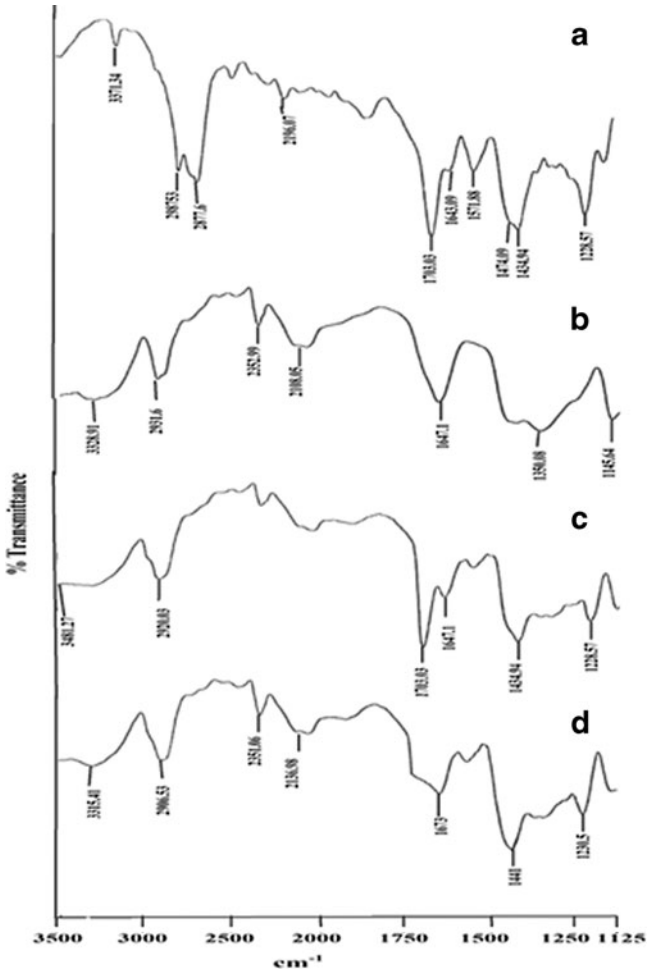

Fig. 5. FT-IR spectra of *a* pure drug LOR, *b* β-CD, *c* physical mixture of LOR and β-CD, and *d* LOR/β-CD complex

Gel Strength

It has been reported that a gel strength of less than 25 is not be able to retain its integrity and can erode rapidly while gels with strength greater than 50 are too stiff that may cause discomfort to the mucosal surfaces or may damage it. The formulations designed displayed gel strength(s) in the range of 26.5–45.6 s (Table III) which is acceptable for nasal delivery as the gel strength values between 25 and 50 are considered sufficiently strong (15). The gel strength was found to be affected by concentration of poloxamer 407 and carbopol 934 P. Higher levels of these resulted in high gel strength.

Ex Vivo Mucoadhesive Strength

Mucoadhesive strength was determined in terms of detachment stress and it was predominantly dependent on the level of carbopol 934 P. Consequently as the level of carbopol 934 P increased, the mucoadhesive strength also increased (Table III). Inclusion of carbopol in the *in situ* gelling systems is favored by its wetting and swelling properties that permit intimate contact of the dosage form with nasal tissue. The contact is established by interpenetration of bioadhesive carbopol 934 P chains with mucin molecules leading to entanglement and formation of weak chemical bonds between entangled chains. Carbopol has very high percentage of (58–68%) of carboxyl groups that undergo hydrogen bonding with sugar residues in oligosaccharide chain of mucin glycoprotein in mucus membrane, resulting in strengthened network between polymer and mucus membrane (25). Stronger the mucoadhesive force is, more it can prevent the gelled solution from coming out of the nose and leading to prolonged retention and increased absorption across mucosal tissues (26). However, excessive mucoadhesive force (*i.e.*, greater than 10,000 dyn/cm^2) gel can damage the nasal mucosal membrane (15). None of our formulations exceeded the upper limit and hence can be visualized as formulations with optimum mucoadhesion properties.

Ex Vivo Permeation

The *ex vivo* permeation study of the *in situ* nasal gels of LOR was done to evaluate the role of β-CD in enhancing the permeation across the nasal mucosa. The *ex vivo* permeation profiles of the formulations (Fig. 7) were used to deduce *ex vivo* permeability parameters (Table IV). Formulations F1, F3, and F5 containing pure drug were not able to achieve

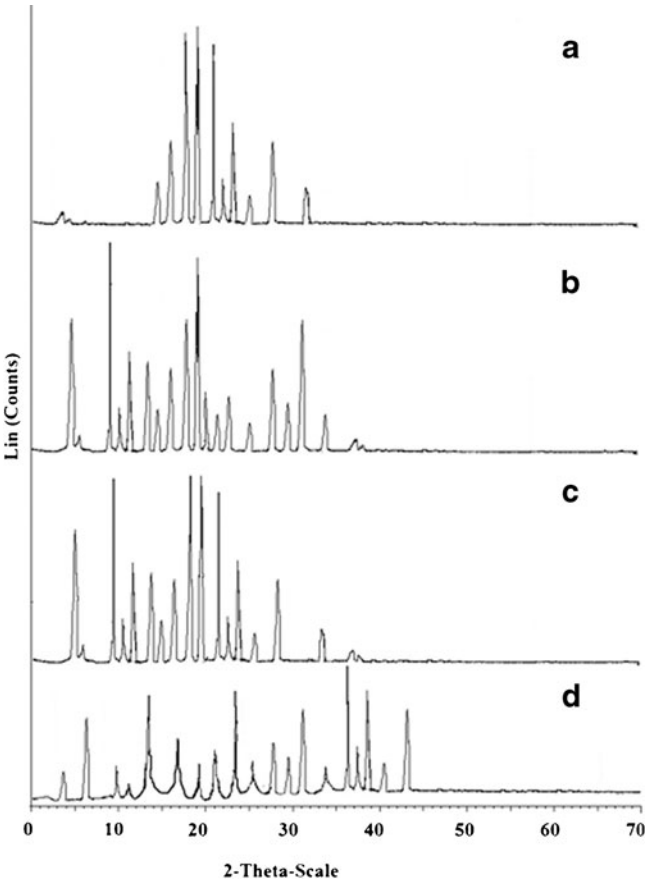

Fig. 6. XRD diffractograms of *a* pure drug LOR, *b* β-CD, *c* physical mixture of LOR and β-CD, and *d* LOR/β-CD complex

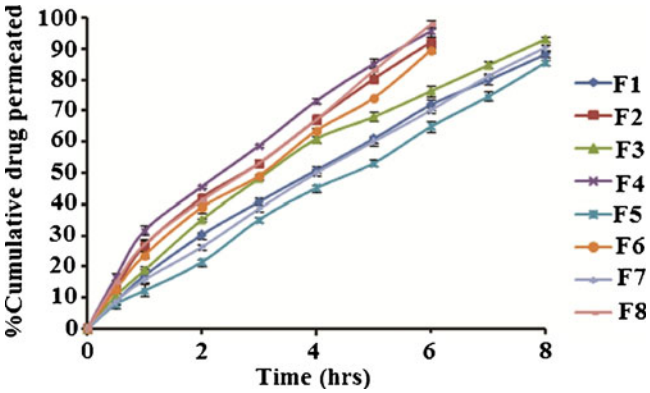

Fig. 7. *Ex vivo* permeation profile of *in situ* nasal gels of LOR (F1-F8) in phosphate buffer pH6.4 for 8 h at 34±0.5°C using Franz diffusion cell

the target flux of 135 μg/cm^2/h. However, F7 reached the target flux, due to high amount(s) of both poloxamer 407 and carbopol 934 P which led to higher permeation of drug. In contrast, the formulations F2, F4, F6, and F8 containing complexed drug were able to reach the target flux attributable to the permeability enhancing property of β-CD.

Consequently, 90% of the drug permeated across the nasal mucosa within 8 h for formulations F1, F3, F5, and F7 while for formulations F2, F4, F6, and F8 it took only 6 h. This can be explained by the dissolving property of β-CD that increased gel porosity and facilitated drug permeation (27, 28). β-CD is also reported to act as permeation enhancer by carrying the drug through the aqueous barrier which exists adjacent to the lipophilic surface of biological membrane (29). Finally, β-CD is also known for its interaction with nasal epithelium thus modifying the tight junctions, lipid, and protein content of the membrane and enhancing the permeation (30). Thus, the cumulative effects of β-CD can be resulted in faster permeation of LOR through nasal membrane.

This study also revealed the importance of Ca^{2+} in enhancing the permeation of LOR across the mucosa. Anionic polymer carbopol is reported to demonstrate permeation enhancing properties as it is able to bind Ca^{2+} of the nasal mucosa modifying the nasal epithelium (18). Thus increase in carbopol 934P levels resulted in increased permeation. When carbopol concentration is increased, it results in increased concentration of ionized carboxyl group which causes conformational changes in the polymeric chain. Also decoiling of the polymer chain occurs due to electrostatic repulsion between the ionized carboxyl groups. During this stage, swelling of the carbopol occurs due to absorption of water from mucus layer which causes intimate penetration into the mucus and hence localizes the formulation in nasal cavity, enhancing the drug concentration gradient across the epithelium. This results in rapid dissolution and diffusion of drug from the gels due to extensive swelling of the ionized carbopol (17). Based on this explanation highest drug permeation of 97.74% in 6 h was demonstrated by F8 (LOR complex, 1% *w*/*v* carbopol and 20% *w*/*v* poloxamer) and least permeation of 64.81% was shown by F5 within 6 h (LOR, 0.5% *w*/*v* carbopol and 20% *w*/*v*

Table III. Evaluation of *In Situ* Nasal Gels of LOR

Formulation code	clarity	pH	Gelling temp (°C)	Gelling time (s)	Viscosity of sol (cps)	Drug content (%)	Gel strength (s)	Mucoadhesive-strength (dyne/cm^2)
F1	Clear	5.75±0.05	33.7±0.47	12.6±0.47	28.34±0.47	77.41±0.40	26.51±0.67	3,626.12±0.34
F2	Clear	5.63±0.01	34.3±0.47	14.6±0.94	27.39±1.25	96.42±0.32	27.82±1.26	3,920.05±0.47
F3	Clear	5.70±0.01	32.6±0.47	10.6±0.94	35.35±0.94	75.21±0.48	33.30±0.94	6,157.67±0.2 3
F4	Clear	5.59±0.01	32.1±0.47	11.3±0.47	34.63±1.24	98.91±0.23	35.61±1.41	6,161.38±0.47
F5	Clear	5.76±0.01	30.7±0.47	8.3±0.47	28.82±0.47	80.32±0.37	38.81±0.87	4,540.61±1.24
F6	Clear	5.64±0.01	30.2±0.23	9.7±0.47	29.09±0.81	92.81±0.54	39.00±0.81	4,847.33±0.46
F7	Clear	5.81±0.01	29.2±0.82	5.7±0.47	43.61±0.47	82.20±0.08	45.61±1.2 7	7,137.64±0.81
F8	Clear	5.34±0.02	28.7±0.47	6.7±0.47	43.36±0.94	97.72±0.59	44.36±0.94	7,676.09±0.97

Table IV. *Ex Vivo* Permeability Parameters of *In Situ* Nasal Gel of LOR Across Sheep Nasal Mucosa

Formulation code	% Cumulative drug permeated (6 h)	Flux (J_{ss}) (μg/cm^2/h)	Permeability coefficients (K_p) (cm/h)	Permeation kinetics
F1	71.89±0.97	113.61	11.36	Zero order
F2	92.23±0.85	199.03	19.90	Higuchi
F3	76.34±1.20	133.51	13.35	Higuchi
F4	95.46±1.12	207.29	20.73	Higuchi
F5	64.81±0.93	132.20	13.20	Zero order
F6	89.67±0.89	190.47	19.04	Zero order
F7	70.23±0.96	141.40	14.14	Zero order
F8	97.74±1.10	211.36	21.13	Zero order

poloxamer). The presence of poloxamer is reported to retard the drug release rate and thus permeation slightly decreases due to reduction in dimension of water channels in the micellar structure (31, 32). As the poloxamer 407 consists of very large amount of micelles in aqueous phase, the incorporated drug may be released by diffusion through gel matrix. Drug release and permeation can also be affected by the gel viscosity, aqueous channel size, and drug distribution between the micelles and the aqueous phase. The increase in poloxamer concentration causes slight increase in viscosity and thus slightly decreases the release of LOR from the gel and thus the permeation (33).

The nasal secretion rate in healthy adults is 5 mm/min while in allergic conditions it decreases to 2.5–3 mm/min and the nasal secretion becomes viscous than the normal secretion (34). This results in increased mucociliary clearance time. On application of *in situ* nasal gel, the nasal secretions are expected to penetrate the gel, dissolute the drug from its β-CD complex, and allow the drug to reach at the interface of the gel and mucosa *via* diffusion. From the interface, the drug will readily penetrate into the mucosal layer and show its effect both, locally and systemically. The secretion helps in the swelling of the gel and facilitates subsequent erosion of the interface of the gel at a constant rate which renders the surface concentration of the drug to be

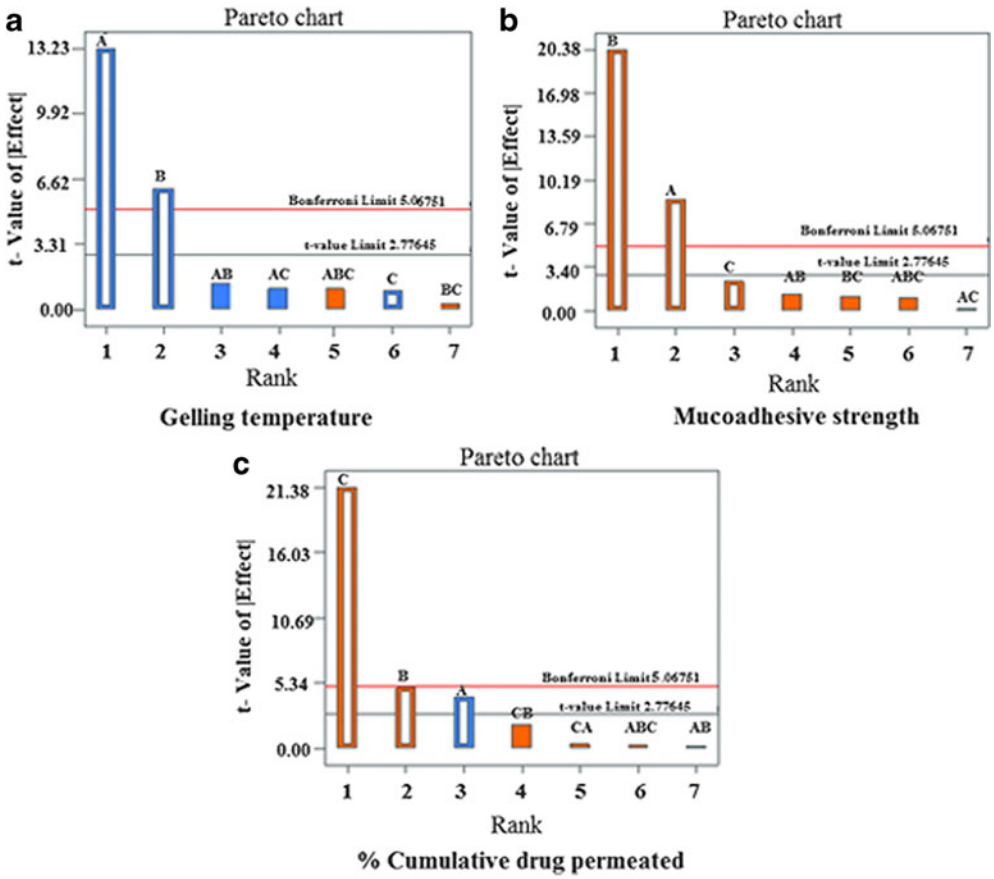

Fig. 8. Pareto charts for analysis of response coefficient significance on the dependent variables; **a** gelling temperature, **b** mucoadhesive strength, **c** percent cumulative drug permeated

Table V. Evaluation of Extra Design Check Point Formulation (F9)

Response parameters	Predicted value	Experimental value
Gelling temperature (°C)	31.40	31.98
Mucoadhesive strength (dyne/cm^2)	5,508.32	5,507.01
%Cumulative drug permeated (6 h)	82.30	81.98

held relatively constant and the drug diffuses out at a constant rate. This is suggested to occur in the case of F8 and the formulation is expected to provide faster onset of action in allergic conditions.

Modeling of the permeation data revealed that most of the formulations followed zero order permeation F2, F3, and F4 which followed the Higuchi model. The permeability coefficient was higher for the gels containing inclusion complexes of LOR-β-CD than the gels made with pure LOR.

Validation of Experimental Design

The selected independent variables namely the concentration of Poloxamer 407, concentration of carbopol 934 P, and the amount of β-CD influenced the gelling temperature, mucoadhesive strength, and percent cumulative drug permeated that is evident from the results in Tables III and IV. To evaluate the effect of each response, the response polynomial coefficients were determined for each dependent variable and each response coefficient was studied for its statistical significance by Pareto charts (Fig. 8). Pareto charts establish *t* value of effect that is studied by two limit lines namely the Bonferroni limit line (*t* value of effect=2.77645) and *t* limit line (*t* value of effect=5.06751). Coefficients, whose *t* value of effect above the Bonferroni line are designated as certainly significant coefficient; coefficients with *t* value of effect between Bonferroni line and *t* limit line are termed as coefficients likely to be significant, while *t* value of effect below the *t* limit line is statistically insignificant coefficient and are removed from the analysis. Thus, insignificant response coefficients were deleted and following significant polynomial response equation(s) for gelling temperature, mucoadhesive strength, and percent cumulative drug permeation (%CDP) were generated.

$$\text{gelling temperature} = 31.40 - 1.74\,\text{A} - 0.80\,\text{B} \quad (5)$$

$$\text{mucoadhesive strength} = 5,508.31 + 42.06\,\text{A} + 1,274.81\text{B} \quad (6)$$

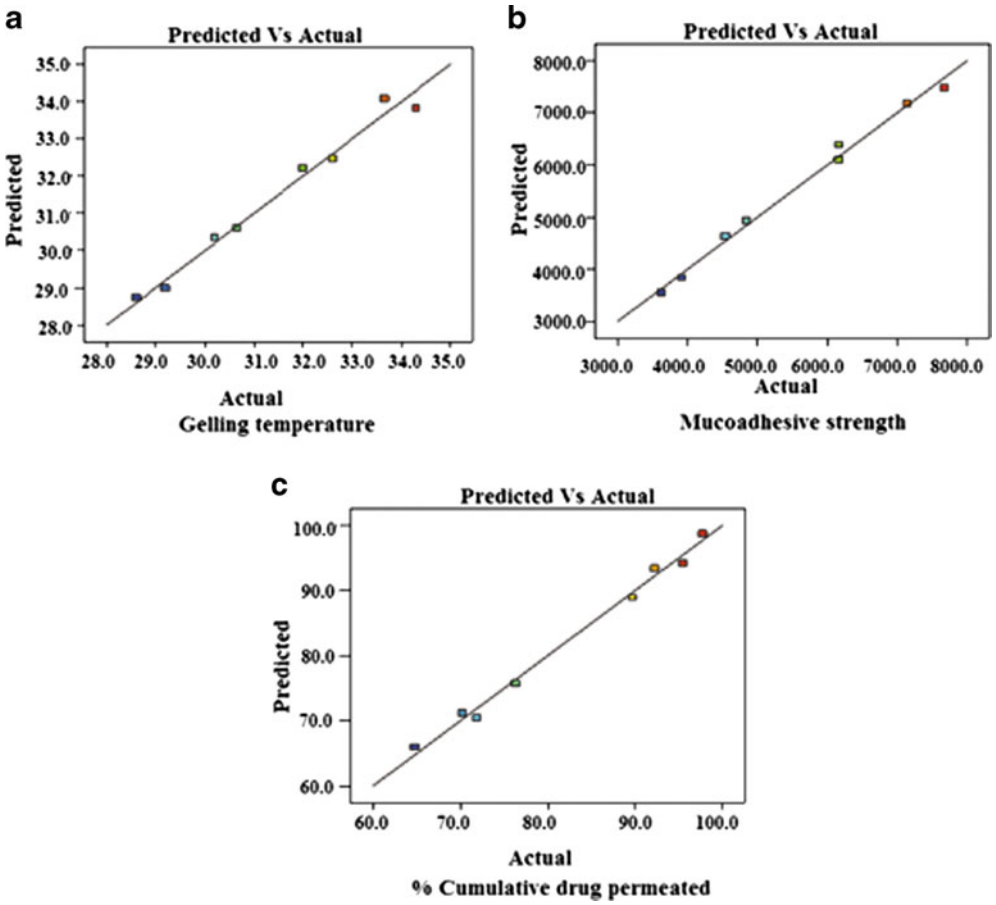

Fig. 9. Predicted *versus* actual values graph for all the dependent variables; **a** gelling temperature, **b** mucoadhesive strength, **c** percent cumulative drug permeated to validate a design

$$\%\,\mathrm{CDP} = 82.30 - 2.25\,\mathrm{A} + 2.65\,\mathrm{B} + 11.48\,\mathrm{C} \qquad (7)$$

These equations were utilized for validation of the experimental design by formulating an extra design checkpoint formulation F9. By utilizing above equations, predicted value(s) for gelling temperature, mucoadhesive strength and %CDP were generated. Experimental values of F9 were determined by formulating and evaluating it, and close resemblance between predicted and experimental values (Table V) indicated validity of the generated model. To further validate the experimental design, graph between predicted *versus* actual for all the eight formulations were obtained for all the dependent parameters (gelling temperature, mucoadhesive strength and %CDP) and straight lines were obtained (Fig. 9). To further analyze the effect of variables on the responses, response surface plots (Fig. 10) were generated that represent the simultaneous effect of any two variables on response parameter taking one variable at constant level. The possible interactions between *AB*, *BC*, and *AC* for each response were also investigated (Fig. 11). Graphically, the interactions are visualized by lack of parallelism in the lines, but in our case case, parallel lines obtained for each interaction term(s) for each response parameter(s) indicated lack of interactions, which in turn indicated that the experimental design has maximum efficiency in estimating main effects. Finally, formulation F8 with least gelling temperature, highest mucoadhesive strength, highest percent cumulative drug permeated after 6 h and maximum desirability factor of 0.88 was selected as optimized formulation.

Histopathological Analysis

Photomicrographs of sheep nasal mucosa after the permeation studies were observed for histopathological changes and compared with the control. No remarkable effects on the microscopic structure of mucosa were observed for the optimized formulation F8. As shown in Fig. 12, neither cell necrosis nor removal of the epithelium from the nasal mucosa was

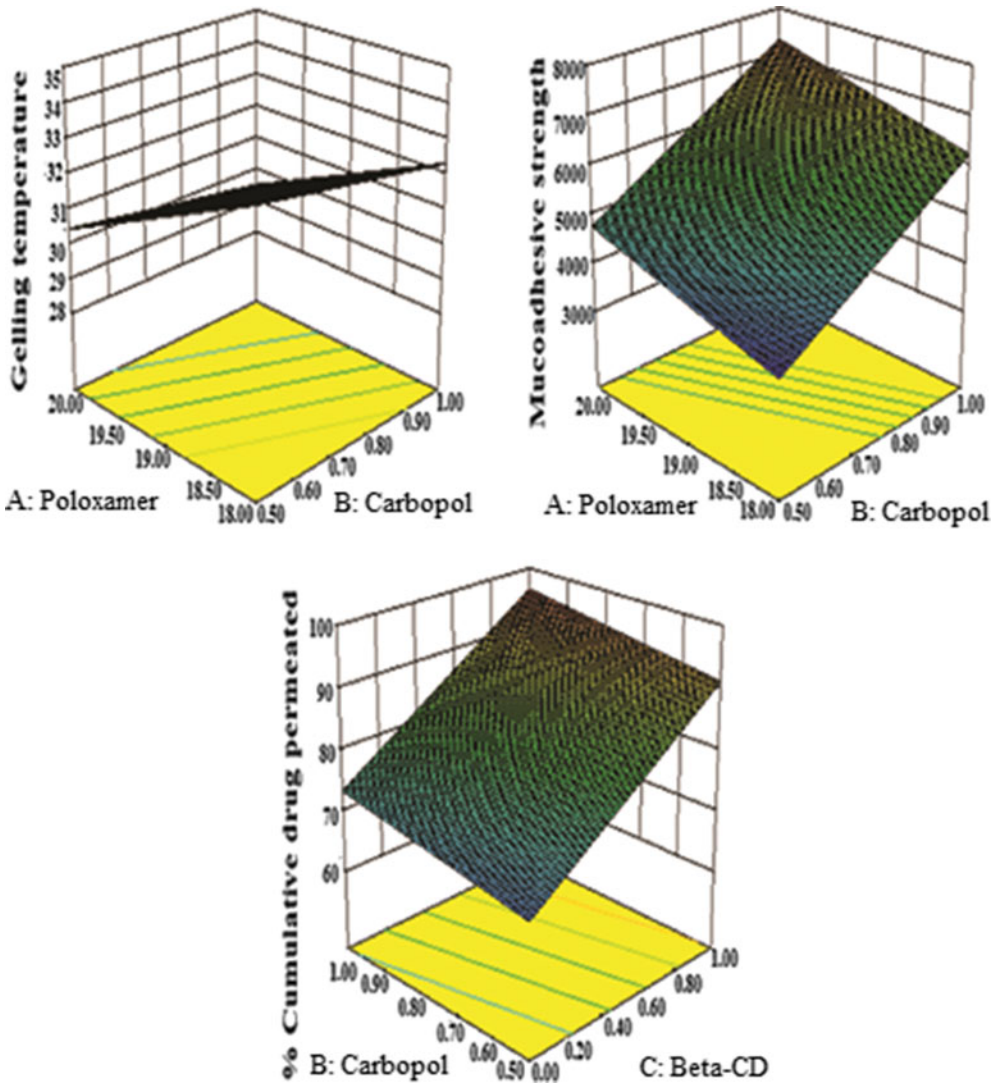

Fig. 10. Response surface plots showing simultaneous influence of independent variables on response parameters of *in situ* nasal gel of LOR within experimental design

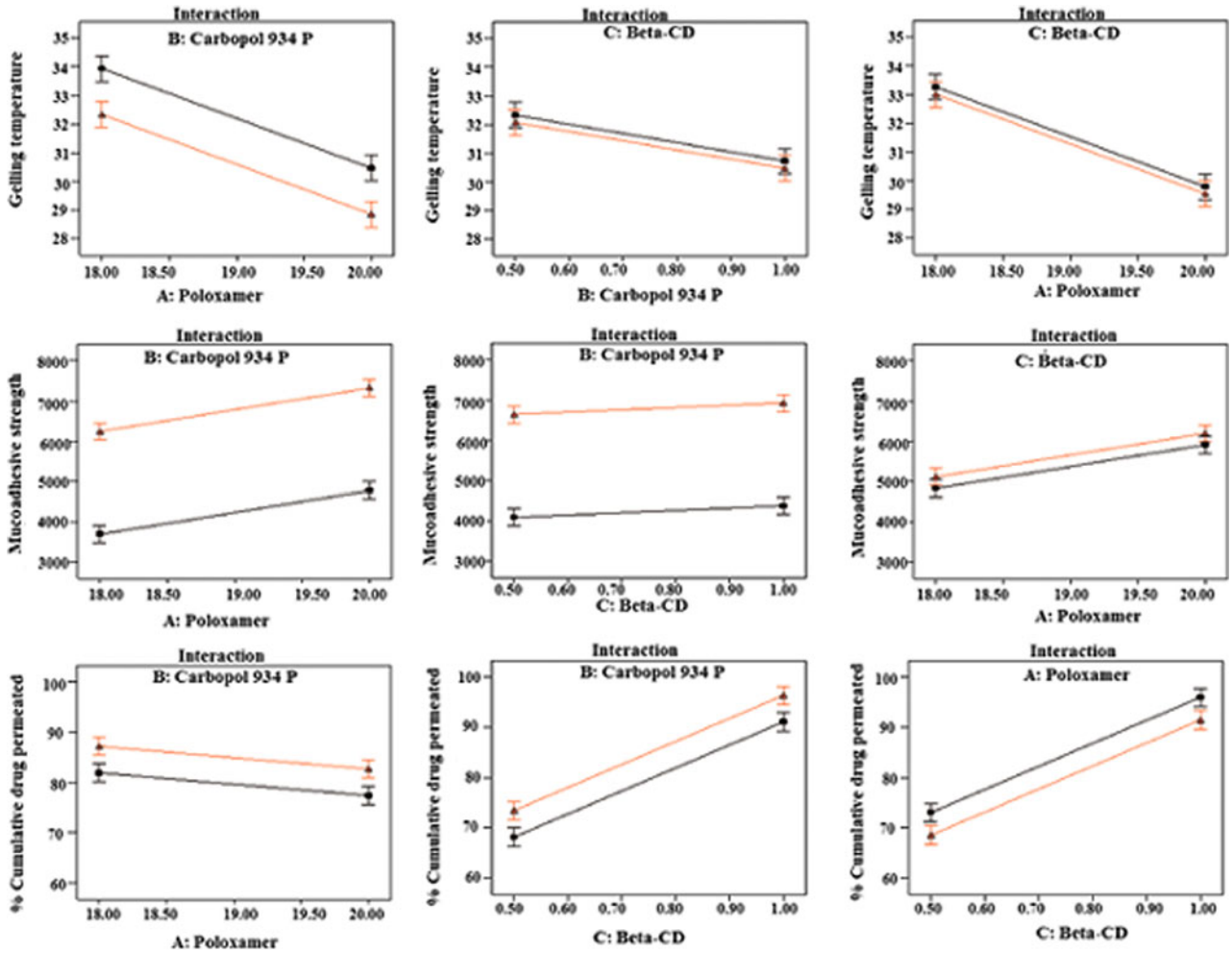

Fig. 11. Interaction studies between variables of *in situ* nasal gel of LOR

observed after permeation of gel. There were no alterations in epithelium layer, basal membrane, and superficial part of submucosal blood vessels when compared with control mucosa. Thus, the *ex vivo* data indicates no adverse local effects. However, local tolerability would need to be reviewed in an *in vivo* study before considering these preparations to be suitable for human use.

Stability

Optimized formulation (F8), exhibited no significance difference ($P<0.05$) in the clarity, pH, drug content, and *ex vivo* permeation characteristics after 3 months (Table VI), which indicate stability of the optimized formulation.

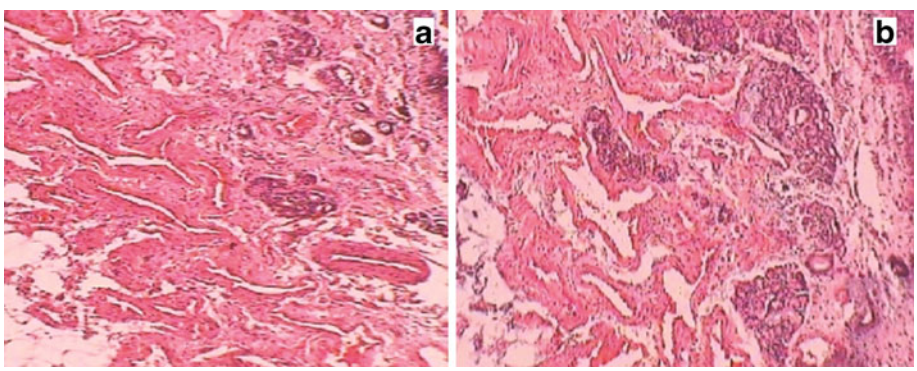

Fig. 12. Histological photomicrographs of sheep nasal mucosa; **a** control mucosa treated with phosphate buffer pH6.4, **b** nasal mucosa after permeation study of *in situ* nasal gel of LOR

Table VI. Stability Study for the Optimized Formulation (F8)

Months	Clarity	pH	Viscosity	Drug content	%CDP (6 h)
0	Clear	5.34±0.017	43.30±0.94	97.72±0.59	95.46±1.20
1	Clear	5.41±0.09	44.30±0.73	96.93±0.74	95.01±0.96
2	Clear	5.48±0.03	45.03±0.82	95.82±0.29	94.12±0.34
3	Clear	5.73±0.07	47.30±0.72	94.72±0.90	94.03±1.40

CONCLUSION

Solubility of loratadine was successfully increased by making its inclusion complex with β-cyclodextrin and was formulated as *in situ* nasal gel. The optimized formulation containing inclusion complex of drug with β-CD achieved the target flux and had sufficient mucoadhesive property to ensure appropriate residence time at the site of application. A controlled permeation of more than 90% drug across the sheep nasal mucosa within 6 h is suggestive of higher therapeutic efficacy and better patient compliance. The formulation was free from cellular damage and stable. However, clinical intricacies need to be reviewed before considering it suitable for human use.

ACKNOWLEDGMENTS

The authors are grateful to Dr. S.K. Garg (Dean and Professor) of Pt. Deen Dayal Upadhaya Pashu Chikitsa Vigyan Vishwavidyalya, Mathura for providing assistance in histopathological study and writing the report of nasal mucosal integrity. The author Reena MP Singh is thankful to AICTE, India, for providing financial assistance during the project.

REFERENCES

1. Menardo J, Horak F, Danzig MR, Czarlewski W. A review of loratadine in the treatment of patients with allergic bronchial asthma. Clin Ther. 1997;19:1278–93.
2. Moffat AC, Osselton MD, Widdop B (2004) Clarke's analysis of drugs and poisons, 3rd ed. Pharmaceutical Press: London 2:1186–1187
3. Borgaonkar PA, Virsen TG, Hariprasanna RC, Najmuddin M. Formulation and *in vitro* evaluation of buccal tablets of loratadine for effective treatment of allergy. Int J Res Pharm Chem. 2011;1:551–9.
4. Shojaei H. Buccal mucosa as a route for systemic drug delivery: a review. J Pharm Pharmaceut Sci. 1998;1:15–30.
5. Merkus FWHM, Verhoef JC, Schipper NG, Martin E. Nasal mucociliary clearance as a factor in nasal drug delivery. Adv Drug Deliv Rev. 1998;29:13–38.
6. Zhou M, Donovan MD. Intranasal mucociliary clearance of putative bioadhesive polymer gels. Int J Pharm. 1996;135:115–25.
7. Martinac A, Grcic JF, Voinovich D, Perissutti B, Franceschinis E. Development and bioadhesive properties of chitosan-ethylcellulose microspheres for nasal delivery. Int J Pharm. 2005;291:69–77.
8. Zaki NM, Awada GA, Mortadaa ND, Abd ElHady SS. Enhanced bioavailability of metoclopramide HCl by intranasal administration of a mucoadhesive *in situ* gel with modulated rheological and mucociliary transport properties. Eur J Pharm Sci. 2007;32:296–307.
9. Higuchi T, Connors KA. Phase-solubility techniques. Adv Anal Chem Instrum. 1965;4:117–212.
10. Schmolka IR. Artificial skin. I. Preparation and properties of Pluronic F-127 gels for the treatment of burns. J Biomed Mater Res. 1972;6:71–582.
11. Choi HG, Shim CK, Kim DD. Development of *in situ* gelling and mucoadhesive acetaminophen liquid suppository. Int J Pharm. 1998;165:33–44.
12. Gupta A, Garg S, Khar RK. Measurement of bioadhesive strength of mucoadhesive buccal tablets: design of *in vitro* assembly. Indian Drugs. 1992;30:152–5.
13. Ramos LA, Cavalheiro ETG. Thermal behavior of loratadine. J Therm Anal Calorim. 2007;87:831–4.
14. Sathigiri S, Chadha G, Lee YHP, Wright N, Parsons DL, Rangari VK, Fasina O, Babu RJ. Physicochemical characterization of Efavirenz-cyclodextrin inclusion complexes. AAPS PharmSciTech. 2009;10:81–7.
15. Mahajan HS, Shah SK, Surana SJ. Nasal *in situ* gel containing hydroxy propyl β-cyclodextrin inclusion complex of arthemeter: development and *in vitro* evaluation. J Incl Phenom Macrocycl Chem. 2011;70:49–58.
16. Nacsa A, Ambrus R, Berkesi O, Szabo-Revesz P, Aigner Z. Water-soluble loratadine inclusion complex: analytical control of the preparation by microwave irradiation. J Pharm Biomed Anal. 2008;48:1020–3.
17. Pedersen NR, Kristensen JB, Bauw G, Ravoo BJ, Darcy R, Larsen KL. Thermolysin catalyses the synthesis of cyclodextrin esters in DMSO. Tetrahedron-Asymmetry. 2005;16:615–22.
18. Majithiya RJ, Ghosh PK, Umrethia ML, Murthy RS. Thermoreversible-mucoadhesive gel for nasal delivery of sumatriptan. AAPS PharmSciTech. 2006;7:E1–7.
19. Kabanov AV, Batrakova EV, Alakhov VU. Pluronic block copolymers as novel polymer therapeutics for drug and gene delivery. J Contr Release. 2002;82:189–212.
20. Bromberg LE, Ron ES. Protein and peptide release from temperature-responsive gels and thermogelling polymer matrices. Adv Drug Deliv Rev. 1998;31:197–221.
21. Kabanov AV, Lemieux P, Vinogradov S, Alakhov V. Pluronic block copolymers: novel functional molecules for gene therapy. Adv Drug Deliv Rev. 2002;54:223–33.
22. Rassing J, Attwood D. Ultrasonic velocity and light scattering studies on polyoxyethylene-polyoxypropylene copolymer PF127 in aqueous solution. Int J Pharm. 1982;13:47–55.
23. Charlton S, Jones NS, Davis SS, Illum L. Distribution and clearance of bioadhesive formulations from the olfactory region in man: effect of polymer type and nasal delivery device. Eur J Pharm Sci. 2007;30:295–302.
24. Patel M, Thakkar H, Kasture PV. Preparation and evaluation of thermoreversible formulations of Flunarizine hydrochloride for nasal delivery. Int J Pharm Pharmaceut Sci. 2010;2:116–20.
25. Efentakis M, Koutlis A, Vlachou M. Development and evaluation of oral multiple-unit and single-unit hydrophilic controlled-release systems. AAPS PharmSciTech. 2000;1:E34.
26. Kunisawa J, Okudaira A, Tsutusmi Y. Characterization of mucoadhesive microspheres for the induction of mucosal and systemic immune responses. Vaccine. 2000;19:589–94.
27. Sangalli ME, Zema L, Maroni A, Foppoli A, Giordano F, Gazzaniga A. Influence of beta-cyclodextrin on the release of poorly soluble drugs from inert and hydrophilic heterogeneous polymeric matrices. Biomaterials. 2001;22:2647–51.
28. Koester LS, Xavier CR, Mayorga P, Bassani VL. Influence of β-cyclodextrin complexation on carbamazepine release from hydroxypropyl methylcellulose matrix tablets. Eur J Pharm Biopharm. 2003;55:85–91.
29. Masson M, Loftsson T, Masson G, Stefansson E. Cyclodextrins as permeation enhancers; some theoretical evaluations and *in-vitro* testing. J Contr Release. 1999;59:107–18.
30. Marttin E, Verhoef JC, Spies F, Van der Meulen J, Nagelkerke JF, Koerten HK, Merkus F. The effect of methylated β-cyclodextrins on the tight junctions of the rat nasal respiratory epithelium: electron microscopic and confocal laser scanning microscophic visualization studies. J Contr Release. 1994;57:205–13.
31. He C, Kim SW, Lee DS. *In situ* gelling stimuli-sensitive block copolymer hydrogels for drug delivery. J Contr Release. 2008;127:189–207.
32. Mortensen K, Pedersen JS. Structural study on the micelle formation of poly(ethylene oxide)-poly(propylene oxide)-poly(ethylene oxide) triblock copolymer in aqueous solution. Macromolecules. 1993;26:805–12.
33. Riccia EJ, Lunardi LO, Nanclares DMA, Marchetti JM. Sustained release of lidocaine from Poloxamer 407 gels. Int J Pharm. 2005;288:235–44.
34. Sun SS, Hsieh JF, Tsai SC, Ho YJ, Kao CH. Evaluation of nasal mucociliary clearance functions in allergic rhinitis patients with technetium-99 m labeled macroaggregated albumin rhinoscintigraphy. Ann Otol Rhinol Laryngol. 2002;111:73–90.